

ISENTROPIC COMPRESSION STUDIES AT THE LOS ALAMOS NATIONAL HIGH MAGNETIC FIELD LABORATORY

D.G. Tasker, C.H. Mielke, G. Rodriguez, and D.W. Rickel
Los Alamos National Laboratory, WX-6, MS J566
Los Alamos, NM 87545, USA

Abstract

A single-turn magnet pulsed power system at the National High Magnetic Field Laboratory (NHMFL) at Los Alamos was originally designed to study actinide samples in extremes of high magnetic field (to 300 Tesla) [1, 2]. A simple modification to the single-turn magnet has converted it to a fast turnaround dynamic high pressure measurement system for Isentropic Compression Experiments (ICE). This paper details the work done including design, theory, modeling and results. The NHMFL system has the advantage of a relatively long-duration current with a ~ 2.3 - μ s rise time, which allows for large sample dimensions, i.e., up to 5 mm thickness, see II.D. The maximum stress is ~ 50 GPa (0.5 Mbar) at the maximum bank voltage (60 kV); higher stresses may be obtained with modifications to the load design.

For the design and predictions of performance of the NHMFL-ICE experiment it is important to have good numerical models. A novel SPICE code simulation was chosen to model all aspects of the experiment, electrical and physical. To this end, accurate dynamic load models were developed to simulate the compression and expansion of the dynamic load at high pressures using shock physics principles.

In this study feasibility of adapting the existing NHMFL capacitor bank for ICE experiments up to 100 GPa is demonstrated. The adaptation saved the expense of building a dedicated capacitor bank yet this new system produces high quality ICE data with a rapid turnaround and very low cost per experiment. A series of proof-of-principle experiments [3] demonstrated the feasibility of the NHMFL-ICE technique; some of the results will be shown here to illustrate the effectiveness of the new technique.

I. INTRODUCTION

The basic techniques and physics of ICE have been described previously [4]. The original ICE technique is due to Asay [5], and a significant body of ICE work has been conducted on the Z-machine at the Sandia National Laboratory. In an ICE experiment, smoothly rising (shock-free) mechanical compression waves are propagated into matched samples of different thicknesses by electromagnetic loading in a planar geometry. A complete EOS isentrope is acquired in one experiment, i.e., continuously from zero up to the peak stress. High

quality isentropic EOS data have been obtained for many materials.

A. Comparison of ICE methods

ICE experiments are performed by depositing megampere currents in the order of 1 μ s from fast capacitor banks [5-10] or by using high explosive techniques [4, 11]; each method has its advantages and disadvantages. The predominant capacitor bank for ICE research is the Z-machine [5] which is capable of delivering currents of tens of MA with rise times of between 100 ns and 600 ns. Pressures of the order of 500 GPa on the Z-machine have been obtained but it is large and expensive to operate. Smaller capacitor banks have been designed specifically for smaller scale ICE experiments, e.g., [7, 10], with good results and these may reach pressures of the order of 50 GPa in approximately 500 ns, but even these machines are relatively expensive to manufacture or purchase.

The explosive techniques developed at LANL can be used to produce ICE data at comparable or greater pressures than those on the Z-machine [12]. At pressures of a few hundred GPa the costs of these explosive experiments are comparable to those of the Z-machine, but the higher pressure experiments would be more expensive. The explosive ICE technique is preferred for: very high pressure experiments; the study of noxious materials that could contaminate capacitor banks and or the buildings that house them; the performance of experiments in remote locations because the explosive experiments are portable and compact.

The NHMFL-ICE technique described in this paper is an excellent method for measuring equations of state (EOS) at pressures up to 1 Mbar. Because many experiments can be performed in one day, the technique promises to provide high quality EOS data at very low cost.

B. Accuracy of the various methods

It should be noted that the accuracy of the ICE technique depends primarily on the accuracy of the diagnostics such as VISAR [13], the quality and precision of sample preparation, high resolution time synchronization, and the uniformity of the magnetic drive. As all ICE techniques use similar diagnostics and sample preparation techniques, the accuracies of ICE data produced by capacitor bank or high explosive techniques are essentially the same [4]. One important advantage of the high explosive technique and some of the smaller

Report Documentation Page		Form Approved OMB No. 0704-0188
Public reporting burden for the collection of information is estimated to average 1 hour per response, including the time for reviewing instructions, searching existing data sources, gathering and maintaining the data needed, and completing and reviewing the collection of information. Send comments regarding this burden estimate or any other aspect of this collection of information, including suggestions for reducing this burden, to Washington Headquarters Services, Directorate for Information Operations and Reports, 1215 Jefferson Davis Highway, Suite 1204, Arlington VA 22202-4302. Respondents should be aware that notwithstanding any other provision of law, no person shall be subject to a penalty for failing to comply with a collection of information if it does not display a currently valid OMB control number.		
1. REPORT DATE JUN 2011	2. REPORT TYPE N/A	3. DATES COVERED -
4. TITLE AND SUBTITLE Isentropic Compression Studies At The Los Alamos National High Magnetic Field Laboratory		5a. CONTRACT NUMBER
		5b. GRANT NUMBER
		5c. PROGRAM ELEMENT NUMBER
6. AUTHOR(S)	5d. PROJECT NUMBER	
	5e. TASK NUMBER	
	5f. WORK UNIT NUMBER	
7. PERFORMING ORGANIZATION NAME(S) AND ADDRESS(ES) Los Alamos National Laboratory, WX-6, MS J566 Los Alamos, NM 87545, USA		8. PERFORMING ORGANIZATION REPORT NUMBER
9. SPONSORING/MONITORING AGENCY NAME(S) AND ADDRESS(ES)		10. SPONSOR/MONITOR'S ACRONYM(S)
		11. SPONSOR/MONITOR'S REPORT NUMBER(S)
12. DISTRIBUTION/AVAILABILITY STATEMENT Approved for public release, distribution unlimited		
13. SUPPLEMENTARY NOTES See also ADM002371. 2013 IEEE Pulsed Power Conference, Digest of Technical Papers 1976-2013, and Abstracts of the 2013 IEEE International Conference on Plasma Science. IEEE International Pulsed Power Conference (19th). Held in San Francisco, CA on 16-21 June 2013, The original document contains color images.		
14. ABSTRACT A single-turn magnet pulsed power system at the National High Magnetic Field Laboratory (NHMFL) at Los Alamos was originally designed to study actinide samples in extremes of high magnetic field (to 300 Tesla) [1, 2]. A simple modification to the single-turn magnet has converted it to a fast turnaround dynamic high pressure measurement system for Isentropic Compression Experiments (ICE). This paper details the work done including design, theory, modeling and results. The NHMFL system has the advantage of a relatively long- duration current with a ~2.3-μs rise time, which allows for large sample dimensions, i.e., up to 5 mm thickness, see II.D. The maximum stress is ~50GPa (0.5 Mbar) at the maximum bank voltage (60 kV); higher stresses may be obtained with modifications to the load design. For the design and predictions of performance of the NHMFL-ICE experiment it is important to have good numerical models. A novel SPICE code simulation was chosen to model all aspects of the experiment, electrical and physical. To this end, accurate dynamic load models were developed to simulate the compression and expansion of the dynamic load at high pressures using shock physics principles. In this study feasibility of adapting the existing NHMFL capacitor bank for ICE experiments up to 100 GPa is demonstrated. The adaptation saved the expense of building a dedicated capacitor bank yet this new system produces high quality ICE data with a rapid turnaround and very low cost per experiment. A series of proof-of-principle experiments [3] demonstrated the feasibility of the NHMFL-ICE technique; some of the results will be shown here to illustrate the effectiveness of the new technique.		
15. SUBJECT TERMS		

16. SECURITY CLASSIFICATION OF:			17. LIMITATION OF ABSTRACT SAR	18. NUMBER OF PAGES 6	19a. NAME OF RESPONSIBLE PERSON
a. REPORT unclassified	b. ABSTRACT unclassified	c. THIS PAGE unclassified			

capacitor banks is their use of parallel plate loads, see section II.A.

C. The NHMFL-ICE facility

The NHMFL-ICE capacitor bank in **Figure 1** has a capacitance of $144 \mu\text{F}$, a maximum charge voltage of 60 kV and a peak discharge current of 4.5 MA. The discharge is sinusoidal with a time to peak of $2.2 \mu\text{s}$. It uses coaxial cables to couple the capacitors to the load and each individual capacitor has its own triggered spark gap closing switch. In its present configuration these closing switches are synchronized to close at the same time. Consequently tailoring the shape of current pulse shape to delay shock-up [12] in the samples is not yet an

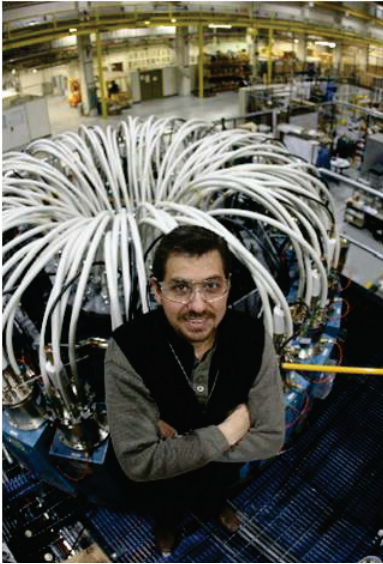


Figure 1. The NHMFL bank showing the cluster of coaxial cables connecting the bank to the load.

option. However, with the slow rise time of this system shock-up is unlikely to be observed; in none of the calculations to date has shock-up been observed.

II. DESCRIPTION OF ICE

A. Stress-equality condition

The basic compression mechanism for ICE is the isentropic magnetic loading of two or more identical samples of different thicknesses, situated on the rear surfaces of a pair of parallel conductors; the complete configuration is called the load, **Figure 2**. *It is essential that the samples are subjected to identical, simultaneous plane wave compressive loads for this technique to be valid.* These samples may be separate from the conductors or may sometimes be integrated into the conductors as one solid piece, i.e., if the samples are good conductors.

In the NHMFL-ICE experiment the load comprises a pair of parallel conductors in a stripline configuration. In contrast, the electrode configuration on the Sandia Z-

machine is a pair of coaxial conductors with a rectangular cross-section. The basic physics of the two configurations is identical, but it has been shown that there are subtleties in the differences of the current flow in the two configurations that affect the accuracy of the techniques [11]; parallel plates are better.

The ICE uses smoothly rising magnetic fields to compress materials to high stresses; this is a ramp or isentropic compression, i.e., without shock. Apart from the shock free compression a significant advantage of the technique is that compression EOS data are obtained at

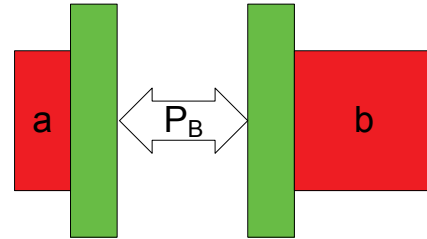


Figure 2. The load. Samples *a* and *b* are attached to the outside of a pair of matched conductors which are subjected to a common magnetic pressure P_B . *a* and *b* differ in thickness by h . The surface velocities of the outside surfaces are measured by VISAR. (The gap d between the conductors has been exaggerated for clarity, see **Figure 3**.)

every stress between the bottom and the top of the ramp in one experiment, i.e., hundreds or thousands of points along the compression curve. By way of contrast, a shock experiment only gives one data point per experiment; so many experiments must be performed to obtain a complete equation of state.

B. Experimental technique

Identical materials of different thicknesses are placed on the rear surfaces of metallic electrical conductors, e.g., copper, **Figure 2**. When the conductor carries current along its inner surface magnetic compression waves are generated which traverse the conductors into the samples. These waves eventually breakout on the rear surfaces of the samples and the velocities of the surfaces are measured by LASER velocimetry such as VISAR or PDV [13, 14].

Consider two equal and opposing currents (I) flowing in the two flat and parallel conductors of **Figure 2** with equal widths (W) and separated by a small distance d . From the Biot-Savart law, the magnetic stresses (B -forces) on the inside surfaces are given by the vector product $\mathbf{P}_B = \mathbf{J} \times \mathbf{B}$, where \mathbf{J} is the linear current per unit width vector (I/W) and \mathbf{B} the magnetic field vector. In the simplest case, when $W \gg d$, \mathbf{J} is uniform and equal and opposite in the electrodes, then the magnitude of the magnetic field on the inside surface of one conductor due the current in the opposing surface is $\frac{1}{2}\mu_0 J$. The magnitude of the common stress normal to the inside surfaces becomes

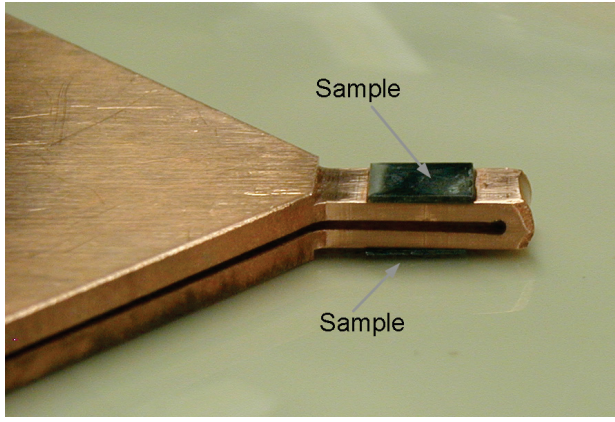


Figure 3. A NHMFL-ICE load. Parallel copper conductors are shown with two tungsten samples on the outside (top and bottom) surfaces.

$$\mathbf{P}_B = \mathbf{J} \times \mathbf{B} \xrightarrow{W \gg d} \frac{1}{2} \mu_0 (I/W)^2 \quad (1)$$

If $J = 10^9$ A/m for example, then $\mathbf{P}_B = 200\pi$ GPa (6.28 Mbar)*. A NHMFL-ICE load is shown in **Figure 3**.

C. Data analysis

Because the thicknesses of a and b in **Figure 2** differ by h , the wave speed $v_L(u)$ may be calculated using *Lagrangian* wave analysis [15]; the times for two *particle* velocity records are measured for each velocity u . In Lagrangian coordinates, h and the density (ρ_0) are constant, so the wave velocity is simply the distance h divided by the difference in arrival times, Δt . The result is a continuous plot of v_L as a function of the particle velocity u ; $v_L(u) = h / \Delta t(u)$.

The change in stress $\Delta\sigma$ is obtained as a function of $v_L(u)$ for each step Δu , working up the curves from zero: $\Delta\sigma = \rho_0 v_L(u) \Delta u$; the complete stress history is then obtained by integration.

The particle velocity (u) is commonly taken to be one-half of the free surface velocity, $u_a = U_a/2$ and $u_b = U_b/2$. However, this is inaccurate at high stresses (i.e., above 50 GPa) because of wave perturbations that occur in the reflection of ramp waves. An exact method is to use the Backward technique [16].

D. Reduction of stress rise time by reflections in the load

The sample dimensions limit the duration of the stress on the load and hence the peak stress. Consider the load shown in **Figure 4**. Compression waves are launched at the left surface of the sample which traverse the sample at the wave velocity until they reach the outside free surface. At that the surface there is only air at atmospheric pressure and therefore little to support a stress rise (see III.G). Consequently, negative going relief waves or rarefactions are initiated at that surface, so that the total

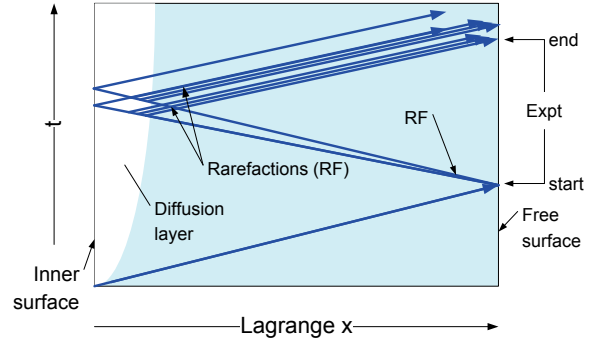


Figure 4. x-t diagram of compression and relief waves travelling in the sample. The left edge of the rectangle is subjected to magnetic loading and compression waves travel left to right and are reflected at the rightmost surface.

stress of the outgoing compression and reflected relief waves is one atmosphere.

These relief waves then travel back to the slit surface, negating the compression on the way, then reflect back to the outside surface as shown. (Note that the reflection from the inside surface is complicated by the presence of the magnetic diffusion layer.) As these rarefaction waves reflect from the slit surface the stress is reduced and this terminates the stress rise on the sample, even though the current flow may not have peaked.

E. Stress-equality condition and end of experiment

As soon as the rarefaction waves arrive back at the slit surface of the *thinnest* sample, the stresses in the two samples are no longer equal. This effectively terminates the experiment, after this time no EOS data may be obtained because the stress equality-condition (section II.A) is violated.

The effect of these relief waves is shown in the calculations of **Figure 5**. The currents and pressures are for copper with the bank charged to 35-kV, the electrode is 10-mm wide and 3 mm thick. After 1.9 μ s the first rarefaction waves arrive reflect back to the inner surfaces and terminate the pressure rise. The peak pressure is reached ~ 400 ns before the peak current. These waveforms were calculated using the design tools described in the next section.

III. DESIGN TOOLS FOR NHMFL-ICE

For the experimental design of the NHMFL-ICE experiment it is important to have good predictive models for the system performance. The tools described here were originally developed for the high explosive ICE experiments [11] and adapted to this NHMFL circuit. A SPICE circuit simulation code [17] was chosen to model all aspects of the experiment, electrical and physical. To this end, accurate dynamic load models were developed to simulate the compression and expansion of the load from shock physics principles.

* μ_0 , free space permeability = 400π nH/m in SI units.

This model, dubbed “*spICE*,” was adapted to the NHMFL-ICE circuit. The capacitor bank and closing switches are modeled by simple static circuit parameters

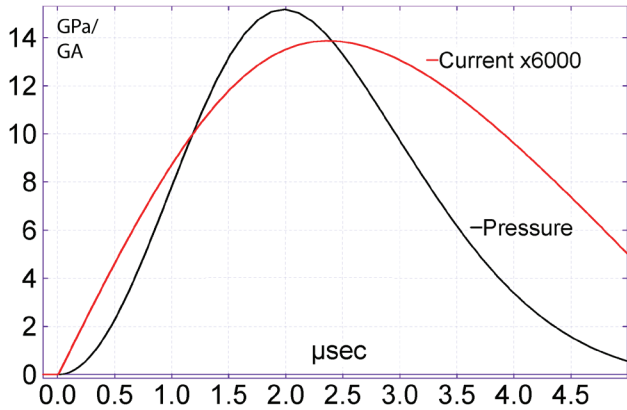


Figure 5. Effect of relief waves on pressure. The peak pressure (15.2 GPa) is at 1.9 μ s after current start yet the peak current (2.3 MA) is at 2.3 μ s. (The current was multiplied by 6000 for display purposes.)

but the load is a complex system dominated by the material dynamics (shock physics) of the materials; it is both time dependent and current dependent.

A. *spICE* circuit simulation for NHMFL-ICE

The NHMFL capacitor bank has a maximum charge voltage of 60 kV and a capacitance of 144 μ F. The connections to the load taper have an inductance of 10 nH and the taper to the load has an estimated inductance of 7.5 nH, see **Figure 6**. X1 is the load simulation circuit which is the only dynamic component of the experiment, Rbank is the resistance of the circuit, XSw1 is a closing switch and VAlload is a zero-voltage supply used as a computational device to monitor current in the load.

The load model provides output values for the inner surface velocities adjacent to the slit, *Up1* and *Up2*; the outer surface velocities which will be observed by the LASER diagnostics, *Ufs1* and *Ufs2*; and the common magnetic pressure, *Pmag*. What follows is a brief description of the circuit model.

B. Parallel plate load compression

As the inner plate separation $d(t)$ increases with time, the inductance of the load increases with time. Consequently, the model must calculate the velocities of inner surfaces (*Up*) to obtain $d(t)$. Also, the rarefactions from the outer surfaces, described above, accelerate the separation of the samples when the rarefactions return to the inner surfaces.

C. Pressure simulation

The pressure distribution on the samples was modeled by solving Maxwell’s equations with a PDE solver [18]. The results showed that the magnetic pressures in the central flat region normal to the surface could be fitted to within 5% with a simple logarithmic function,

$$P_y = \frac{1}{2} \mu_0 \left(0.11853 - 0.21641 \times \ln \overline{d/W} \right) J^2.$$

The movement (separation) of the electrodes was obtained from the SPICE calculations described below, then the PDE calculations were by repeated for the different load separations. In these calculations it was assumed that the conductivity of the conductors was constant, which is an approximation. Calculations for higher pressure experiments must take the variation of conductivity with pressure and temperature into account.

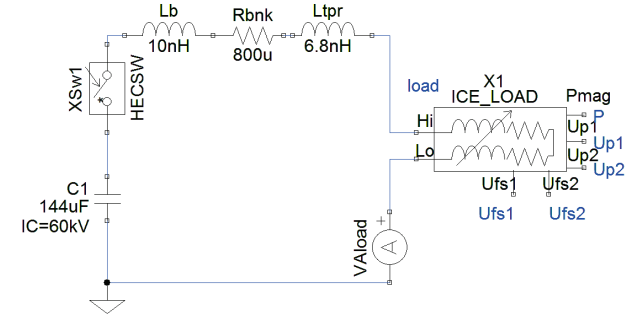


Figure 6. *spICE* simulation of the NHMFL circuit. Here the only dynamic circuit element is the load (X1).

D. Load inductance

The load inductance $L(t)$ of the NHMFL-ICE experiment was calculated according to the following equation where $K(W/d)$, a function of W/d , is an analytic solution for the correction factor for separation and l is the length of the conductors (the results are identical to published $K(W/d)$ data [19]). $K = 1$ when W/d is large and $K = \frac{1}{2}$ when $W/d = 1$.

$$L(t) = \mu_0 K_{(W/d(t))} \times \left(\frac{d(t)}{W} \right) l$$

E. Transmission line analog

To model the wave propagation and reflection in the expanding electrodes an electromechanical analog was employed, i.e., the sample was modeled with an electrical transmission line. Mechanical particle velocity was equated to electrical current and mechanical pressure was equated to electrical voltage. Each sample with its free surface was treated as a short-circuited transmission line. To date the effects of the magnetic diffusion layer have not been modeled. In practice this approximation has little effect on the accuracy of the predictions.

The electrical impedance of the transmission line was equated to the acoustic wave impedance of the samples, $\rho_0 \times v_L(P)$, i.e., the product of the initial density and the velocity v_L which is pressure dependent. No published or commercial SPICE models for transmission lines that have voltage (pressure analog) dependent velocities were available. Consequently, a number of different techniques were tried to simulate such a transmission line; most attempts were unsuccessful because those models became numerically unstable. The best solution was found to be a

16-stage lumped RCL circuit model for the transmission line where the capacitance of each stage was voltage dependent, $C = C(V)$, i.e., a function of voltage (pressure), **Figure 7**. Note that the load (R_{load} and L_{load}) is a short

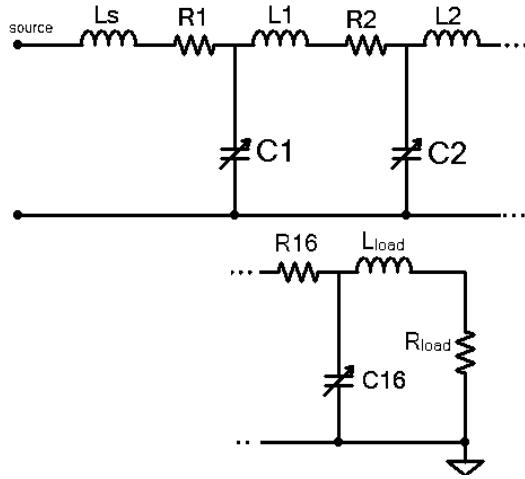


Figure 7. 16-stage variable velocity transmission line. All 16 inductances are equal, as are the 16 resistances. Each capacitor is independent of the others and controlled by the voltage across it.

circuit for a simple one-piece electrode and sample in air, but the load could be a second transmission line representing the sample in a two- or three-piece electrode-load-window configuration.

The variable capacitance $C(V)$ was set to a function of voltage which mirrored the known velocity versus pressure relationship for the metal of interest, copper or tungsten here. For example, from the isentrope of copper we know the Lagrangian wave velocity, v_l , in OFHC copper as a function of pressure. It can be expressed as a fourth order polynomial up to 100 GPa, where the a_i coefficients for $i = 0$ to 4 are: 3945.18; 8.05451×10^{-8} ; -5.59069×10^{-19} ; 4.51653×10^{-30} ; and -1.56767×10^{-41} .

$$v_l = \sum_{i=0}^4 a_i P^i$$

Equations (2) summarize the relationships and their analogs where τ is the delay of the transmission line which is equivalent to the sample thickness λ divided by the wave velocity.

$$\begin{aligned} v_L &= f(V) \equiv f(P) \\ Z &= \sqrt{L/C(V)} \equiv \rho_0 v_L \\ \tau &= N\sqrt{LC(V)} \equiv \lambda / v_L \\ L &\equiv \frac{\lambda \rho_0}{N} \\ C(v_L) &\equiv \frac{1}{L} \left(\frac{\lambda}{N v_L} \right)^2 \end{aligned} \quad (2)$$

The *spICE* calculations shown here were for a uniform electrode and sample configuration. In other words, the conductor and sample were of the same material, either copper or tungsten throughout, and therefore only one

transmission line was necessary to model wave reflections in the load. For the last two experiments in the series, tungsten samples were attached to the outside of the copper electrodes. To model these required an additional transmission line was added for each the samples. Additional transmission lines may be added to simulate windows that are often used in ICE experiments.

F. *spICE* calculation of the NHMFL-ICE load response

The *spICE* model was used to predict the results of the NHMFL-ICE experiments. The plots in **Figure 8** are the experimental results and predictions for a copper sample which was *nominally* 3.175 mm thick, and 10 mm wide. Note the ringing of the surface velocities in the figure which is caused by the multiple wave reflections in the load. The stress-equality condition is not valid after the arrival of the first reflection, see Figure 4, so the EOS data gathering portion of the experiment would have ended at $\sim 1.8 \mu\text{s}$. The calculations appear close to the measured surface velocities up to $3.2 \mu\text{s}$ when there is a significant divergence of the velocities; the cause is unknown but may have been due to air flash, see below. Before that

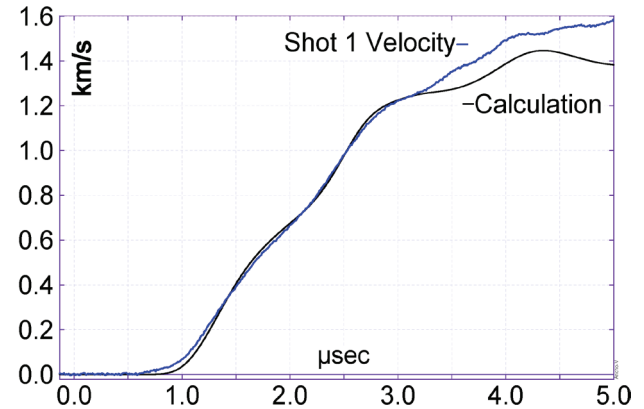


Figure 8. Comparison of predictions (black) of surface velocity and VISAR results (blue) of the first experiment for a 3.175-mm thick copper sample, 1 cm wide, bank voltage 35 kV.

time the differences between experiment and calculation can easily be explained by the estimated errors in dimensional measurement (a few percent). Clearly the *spICE* simulation of these ICE experiments produces good results. Note that any errors in the predictions would not affect the accuracy of the EOS data that is subsequently obtained from the data using the Backward method.

G. Air flash

The proof-of-principle experiments were performed in air for economy; hence air flash may have affected the velocimetry measurements. These errors will be eliminated by performing future experiments in vacuum.

IV. SUMMARY

The NHMFL-ICE technique has been shown to be an excellent method for measuring high pressure EOS data at pressures approaching 100 GPa. Because a complete EOS can be obtained in one experiment from zero to the peak pressure, and because many shots can be fired in one day, the technique promises to provide high quality EOS data at relatively low cost. The low cost makes ICE accessible to a broader scientific community. For example, the performance of ICE on geological materials becomes economically viable.

As the rise time of the NHMFL capacitor bank is relatively long, circa 2 μ s, the sample dimensions are relatively large, i.e., up to 5 mm thickness. Thicker samples improve the accuracy of the technique [11].

Four successful experiments were performed which demonstrated the feasibility of the NHMFL-ICE technique. The measured velocities were close to the predicted values, i.e., within the estimated errors in metrology.

As the NHMFL capacitor bank is compact it is transportable. With it, ICE experiments could be performed at such locations as: the Nevada Test Site; MaRIE, the proposed LANL Matter-Radiation Interactions in Extremes facility; the LANL proton radiography facility; the ANL Advanced Photon Source.

V. ACKNOWLEDGEMENT

The authors are indebted to C. Barnes, T. Taylor, D. Watkins, and R. Martineau of Los Alamos National Laboratory for supporting this work.

VI. REFERENCES

- [1] S. E. Sebastian, et al., "Metal-insulator quantum critical point beneath the high T_c superconducting dome," *Proceedings of the National Academy of Sciences*, vol. 107, pp. 6175-6179, April 6, 2010.
- [2] A. M. Alsmadi, et al., "Complex conductivity of UTX compounds in high magnetic fields," *Journal of Applied Physics*, vol. 105, pp. 07E108-3.
- [3] D. G. Tasker, C. H. Mielke, G. Rodriguez, and D. G. Rickel, "A Simple Isentropic Compression Experiment (ICE) Machine," presented at the APS Shock Conference, American Physical Society, Shock Compression of Condensed Matter, Topical Group, Chicago, 2011.
- [4] D. G. Tasker, J. H. Goforth, and H. Oona, "High Accuracy Isentropic Compression Studies With High Explosive Pulsed Power," presented at the Proceedings IEEE Pulsed Power Conference, Albuquerque, NM, USA, 2007.
- [5] J. R. Asay, "Isentropic compression experiments on the Z accelerator," in *Topical Conference on Shock Compression of Condensed Matter Snowbird*, Utah (USA), 1999, pp. 261-266.
- [6] C. Deeney, J. P. Davis, C. A. Hall, M. D. Knudson, and T. J. Vogler, "High-Pressure Isentropic Compression Experiments on the Sandia Z Accelerator," in *Plasma Science, 2005. ICOPS '05. IEEE Conference Record - Abstracts. IEEE International Conference on*, 2005, pp. 103-103.
- [7] T. Ao, "Quasi-isentropic Compression of Materials Using the Magnetic Loading Technique," presented at the Shock Compression of Condensed Matter, Nashville, TN, 2009.
- [8] T. Ao, J. R. Asay, S. Chantrenne, M. R. Baer, and C. A. Hall, "A compact strip-line pulsed power generator for isentropic compression experiments," *Review of Scientific Instruments*, vol. 79, pp. 013903-16.
- [9] C. Sun, et al., "Magnetically Driven Isentropic Compression and Flyer Plate Experiments Using a Capacitor Bank," presented at the Shock Compression of Condensed Matter, Waikoloa, Hawai'i, 2007.
- [10] G. Avriault, et al., "GEPI: a compact pulsed power driver for isentropic compression experiments and for non shocked high velocity flyer plates," in *14th IEEE International Pulsed Power Conference. Digest of Technical Papers. PPC-2003*, pp. 913-916 Vol.2.
- [11] D. G. Tasker, "Megabar Isentropic Compression Experiments (ICE) Using High Explosive Pulsed Power (HEPP)" Doctor of Philosophy Department of Electronic and Electrical Engineering Loughborough University Loughborough, UK, 2006.
- [12] J. H. Goforth, et al., "Design of High Explosive Pulsed Power Systems for 20 MB Isentropic Compression Experiments," presented at the Ninth International Conference on Megagauss Magnetic Field Generation and Related Topics MG-IX, St. Petersburg (RU), 2002.
- [13] L. M. Barker and R. E. Hollenbach, "Laser Interferometer for Measuring High Velocities of any Reflecting Surface," *Journal of Applied Physics*, vol. 43, p. 4669.
- [14] O. T. Strand, D. R. Goosman, C. Martinez, T. L. Whitworth, and W. W. Kuhl, "Compact system for high-speed velocimetry using heterodyne techniques," *Review of Scientific Instruments*, vol. 77, pp. 083108-8.
- [15] J. B. Aidun and Y. M. Gupta, "Analysis of Lagrangian gauge measurements of simple and nonsimple plane waves," *Journal of Applied Physics*, vol. 69, pp. 6998-7014.
- [16] D. Hayes, "Backward Integration Of The Equations Of Motion To Correct For Free Surface Perturbations," Sandia National Laboratories, Albuquerque, NM SAND2001-1440, May 2001.
- [17] Penzar, "TopSPICE/Win32," 7.19 ed: Penzar Development, P.O. Box 10358, Canoga Park, CA 91309, U.S.A., 2009. A generic SPICE code.
- [18] R. G. Nelson, "FlexPDE Professional ", 5.0.16 ed. Sunol, CA: PDE Solutions Inc, 2007.
- [19] H. Knoepfel, *Magnetic Fields*: John Wiley & Sons Inc., 2000.